Seismic Control of Continuous Bridges Using Variable Radius Friction Pendulum Systems and Viscous Fluid Dampers

A. Krishnamoorthy

Department of Civil Engineering, Manipal Institute of Technology, Manipal, 576 104, Karnataka, India

(Received 28 December 2012; revised 19 September 2013; accepted 5 March 2014)

This paper investigates the performance of a variable radius friction pendulum system (VRFPS) with supplementary damping using viscous fluid dampers (VFD) to control the seismic response of bridges. A VRFPS is similar to a frictional pendulum system (FPS), but the curvature of the sliding surface is varied, and it becomes the function of the sliding displacement. The bridge is seismically isolated with a VRFPS between the superstructure and the pier, and a VFD is added between the abutment and superstructure. Effectiveness of the proposed system is studied for a three-span continuous bridge isolated with a VRFPS and VFD hybrid system. The performance of a proposed system is compared to a corresponding performance of a hybrid system consisting of a conventional FPS with a VFD. The results of the numerical simulation showed that supplementary damping reduces the seismic response of the isolated bridge. Further, a hybrid system consisting of a VRFPS and a VFD is found to be more effective than a FPS and a VFD hybrid system for seismic control of bridges.

1. INTRODUCTION

Bridges are susceptible to damage when subjected to major earthquakes. The damage to the bridge structure occurs primarily in the piers, which results in the collapse of the bridge super structure. In recent years, seismic isolation devices such as rubber bearings or sliding bearings have been used to improve the seismic response and to reduce the damage of bridges for both new and retrofitting applications. These devices are placed between the superstructure and pier. The friction pendulum system (FPS) proposed by Zayas et al.[1] is recognized as an effective isolation device to reduce the seismic effects of buildings and bridges. In this system the sliding and restoring mechanisms are integrated in one unit in which the sliding surface takes a spherical shape.[2] However, the restoring stiffness, which is proportional to the curvature of the sliding surface will inevitably introduce a constant isolation frequency to the isolated structure.[3] This frequency remains constant during the earthquake ground motion due to the spherical sliding surface. A resonant problem may occur when the structure resting on the FPS is subjected to near-fault earthquake ground motions characterized by low frequency and high intensity. In one of the approaches, to overcome this problem, a sliding surface with variable frequency has been suggested.[2–4] In this system, the shape of the sliding surface of the FPS is made non-spherical by varying the curvature of the sliding surface with isolator displacement. These isolators are found to be effective in reducing the forces transferred to the structure at all intensities of excitations without showing any resonance problems. However, the sliding surface of these isolators is flatter than the FPS system. This induces large sliding displacement for low frequency and high intensity earthquakes, resulting in expensive loss of space for a seismic gap. In another approach, to overcome the resonance problem, various additional seismic control devices such as passive viscous fluid dampers[5,6] and active or semi-active variable stiffness or variable damping devices have been augmented[7–11] to the FPS or rubber bearings. Although, the active or semi-active devices by varying the properties like stiffness or viscosity are found to be more effective compared to passive devices, such systems are relatively complex since they require special hardware, sensors, and constant maintenance. On the other hand, passive devices are easy to maintain since they do not require any additional power and sophisticated equipment. Several analytical and experimental studies carried out on isolated buildings and bridges demonstrated a reduction in bearing displacement when additional passive damping devices are added to the FPS or rubber bearings. However, the major drawback of passive dampers with the FPS is their inability to adjust the parameters during the earthquake in response to seismic excitations. To overcome this problem, a FPS with a variable frequency is proposed in the present study instead of a FPS with a constant frequency. In the case of a variable frequency FPS, the frequency varies in response to seismic excitation due to the geometry of the isolator without the need of any external power. A new isolator known as a variable radius friction pendulum system (VRFPS) is proposed, and its effectiveness is investigated when additional passive damping using a viscous fluid damper (VFD) is added. A VRFPS isolator is used to overcome the resonance problem of the FPS associated with near-fault characteristics, and an additional passive damping device is used to reduce the sliding displacement of the isolator. Krishnamoorthy[12] studied the effectiveness of the VRFPS with a VFD for seismic isolation of space-frame structures. In this study, the effectiveness of the proposed isolator with a VFD is investigated to control the seismic response of a continuous bridge. The mechanical behaviour of a VRFPS is similar to that of a FPS. The difference between the VRFPS and a FPS is that the radius of the curvature is constant in the case of a FPS whereas it varies with the sliding displacement in the case of the VRFPS. For the pro-

posed isolator, the radius of the curvature along the sliding surface is varied using an exponential function. A VFD is placed between the abutments and superstructure, and a VRFPS is placed between the pier and superstructure. To study the effectiveness of the proposed system, the response of the bridge isolated with a VRFPS and a VFD system is compared with the response of a bridge isolated with a FPS and a VFD system under similar conditions.

2. GEOMETRY OF THE PROPOSED SLIDING SURFACE

In the case of a conventional FPS, the radius of the curvature, R, of the isolator is constant. Due to this, it may encounter a resonance problem at a low frequency. In order to overcome this limitation, an isolator with a varying radius of curvature along the sliding surface is proposed. Two similar devices, a variable frequency pendulum isolator (VFPI) and a variable curvature friction pendulum system (VCFPS) have been proposed respectively by Pranesh and Sinha[2] and Tsai et al.[4] The sliding surface of the VFPI is based on the expression of an ellipse, and the concave sliding surface of the VCFPS is based on subtracting a specific function from the expression of the FPS sliding surface. However, varying the radius exponentially with the sliding displacement proposed in this study can get the equation to describe the concave sliding surface of the VRFPS. The geometry of the isolator proposed in this study is similar to the geometry proposed by Krishnamoorthy[12] to isolate the space frame structure. The geometry of the VRFPS is chosen in such a way that its radius is similar to the radius of the FPS system at the centre of the sliding surface, and it increases with the sliding displacement and becomes infinity at a large sliding displacement. An expression to vary the radius exponentially with sliding displacement is found to be satisfactory in meeting the above requirement. For the proposed sliding surface, the radius of the curvature is a function of the sliding displacement x, and is given by the expression

$$R(x) = C\left(\exp\left(x\right) - 1\right) + R. \tag{1}$$

In the above equation, the sliding displacement x is expressed in meters, and C is the parameter to describe the variation of curvature of the concave surface. R is the radius of curvature, in meters, at the centre of VRFPS (at $x = 0$).

For a mass, m, sliding on a smooth curved surface of geometry, $y = f(x)$, restoring force, F_R, can be expressed by the following two equations as proposed by Pranesh and Sinha:[2]

$$F_R = mg\frac{dy}{dx} \tag{2}$$

and

$$F_R = m\omega_r^2 x; \tag{3}$$

where, ω_r is the isolator frequency and is equal to $\sqrt{\frac{g}{R}}$ (R, is the radius of curvature of the sliding surface). For the proposed isolator, radius R, and isolator frequency, ω_r, is varying and is a function of sliding displacement, x.

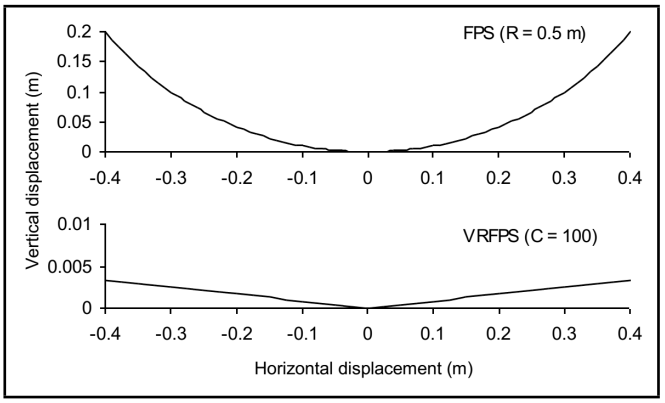

Figure 1. Geometry of VRFPS and FPS isolators.

From Eqs. (2) and (3):

$$\frac{dy}{dx}(x) = \frac{x}{R(x)}, \quad \text{i.e.} \quad \frac{dy}{dx}(x) = \frac{x}{C\left(\exp\left(x\right) - 1\right) + R};$$
$$y(x) = \int \frac{x\,dx}{C\left(\exp\left(x\right) - 1\right) + R}. \tag{4}$$

The above equation defines the geometry of the sliding surface. The vertical displacement, y, at sliding displacement, x, can be obtained by integrating the above equation numerically. Figure 1 shows the sliding surface of the VRFPS with the initial radius $R = 0.5$ m and $C = 100$. The sliding surface of the FPS with a constant radius $R = 0.5$ m is also shown in the same figure. The radius of curvature of the VRFPS increases as compared to the FPS while increasing the sliding displacement. Also, as evident from Fig. 1, the VRFPS is relatively flatter than the FPS.

3. ANALYTICAL MODELLING

Figure 2 shows the three-span continuous bridge considered for the study. The bridge is seismically isolated with the VRFPS between the superstructure and the pier and with the VFD between abutments and superstructure. The VRFPS is modelled as a fictitious spring of stiffness, k_b. The super structure between the supports, each pier, and each sliding bearing are considered as an element interconnected at the joints. One end of the spring is connected to the superstructure while the other end is connected to the top of the pier. When the system is in a non-sliding phase, the stiffness of the fictitious spring is considered as a large value so that the relative displacement between the super structure and the pier at the interface is zero whereas when the system is in sliding phase, the stiffness of the fictitious spring is considered as zero to allow the sliding of the super structure at the interface. The super structure, pier, and isolator are modelled as an element with one horizontal degree of freedom at each node. The stiffness matrix of the super structure, the stiffness of the pier, and the stiffness of the sliding bearing, k_b, are added to obtain the stiffness matrix, K, of whole bridge structure. The mass of the super structure and pier is lumped at the nodes. The overall dynamic equation of the equilibrium for the bridge structure can be expressed in matrix notation as

$$[M]\{\ddot{u}\} + [C]\{\dot{u}\} + [K]\{u\} = \{F(t)\}; \tag{5}$$

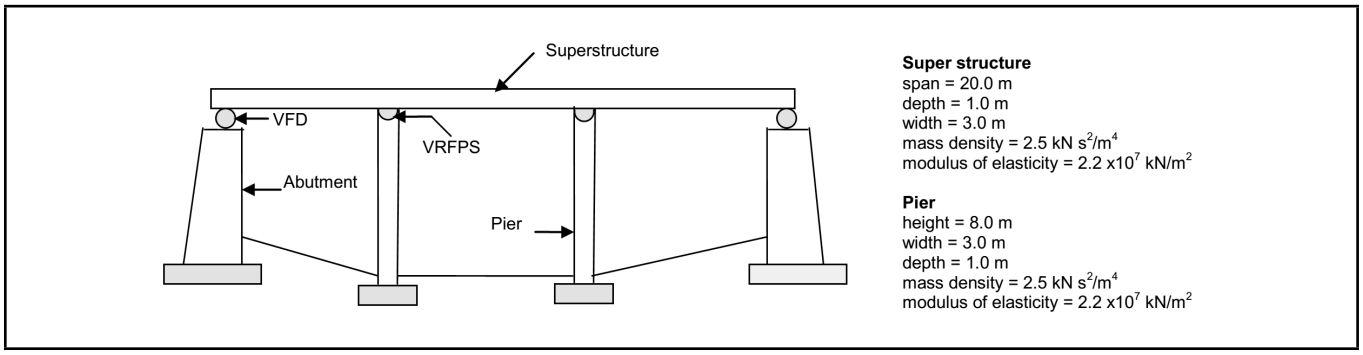

Figure 2. Three-span continuous bridge considered for the study.

where $[M]$ and $[C]$ are the mass matrix and damping matrix, respectively; $\{\ddot{u}\}$, $\{\dot{u}\}$, $\{u\}$ are the acceleration, velocity, and displacement vectors relative to the ground at nodes; $\{F(t)\}$ is the nodal load vector; and $\{u\} = \{u_1, u_2, u_3, \ldots, u_n\}$, where n is the number of nodes.

The nodal load vector $\{F(t)\}$ for the non-sliding phase, is obtained using the equation

$$\{F(t)\} = -[M]\{I\}\ddot{u}_g(t). \tag{6}$$

Whereas, for the sliding phase,

$$\{F(t)\} = -[M]\{I\}\ddot{u}_g(t) + \{F_r\}. \tag{7}$$

In this case, $\{I\}$ is the influence vector, and $\ddot{u}_g(t)$ is the ground acceleration. $\{F_r\}$ is the nodal load vector due to the isolator force. This force mainly consists of two components: i) restoring force due to the component of the weight of the superstructure on each isolator and ii) the frictional force. Frictional force, F_s, is the maximum frictional resistance offered by the sliding surface and is equal to the product of the weight of the superstructure, W, on each isolator and the friction coefficient μ (i.e. $F_s = \mu W$). The restoring force is the product of the stiffness of the isolator (due to gravity) and relative displacement between the super structure and the pier.

At the degrees of freedom corresponding to the super structure,

$$F_r = -k_r u_r - F_s \operatorname{sgn}(\dot{u}_r); \tag{8}$$

and at the degrees of freedom corresponding to the pier,

$$F_r = k_r u_r + F_s \operatorname{sgn}(\dot{u}_r); \tag{9}$$

where k_r is the stiffness of isolation provided through its gravity ($k_r = m\frac{g}{R(x)}$). u_r and $\dot{u}_r$ are the displacement and velocity of the superstructure relative to the pier (i.e., $u_r = u_{\text{super structure}} - u_{\text{pier}}$); sgn denotes the signum function.

4. NUMERICAL EXAMPLES

An example of a three-span continuous bridge has been considered in order to study the effectiveness of the proposed hybrid isolator system as shown in Fig. 2. The bridge is isolated between the pier and the superstructure using the VRFPS isolator, and a supplementary damping is provided using the VFD between the abutment and the pier. Geometric and material properties considered for the study are shown in Fig. 2. The time period of the non-isolated bridge is equal to 0.47 s. The damping ratio of the bridge is 5 percent, and the coefficient of friction of the sliding material is 0.05. The isolator constant, $C = 100$ and initial radius, $R = 0.5$ m are considered for the proposed VRFPS isolator. For comparison, the FPS with a radius 0.5 m (time period, $T = 1.43$ s) is considered. Acceleration records used for numerical simulation are the three commonly used earthquake ground motions. They are:

i) N-S component of El Centro earthquake (Imperial Valley, 1940)

ii) E-W component of Northridge earthquake (Newhall, 1994)

iii) Chi-Chi earthquake at station TCU075 (Taiwan, 1999)

The wave forms of these three records are shown in Figs. 3a, 3b, and 3c. The first record of the El Centro earthquake shown in Fig. 3a has been used to simulate the response of many earthquake engineering structures. Since the El Centro earthquake has no long period characteristics, it is used to represent a far-field earthquake in this study. On the other hand, the Northridge and Chi-Chi earthquakes shown in Figs. 3b and 3c exhibit a long period pulse like wave forms, and hence, these two earthquakes are used in this study to represent the near-fault earthquakes. In order to show the effectiveness of the VRFPS to the earthquake ground motion, the base shear at the pier foot along with the sliding displacement of the superstructure and the residual displacement of the isolator are examined. The base shear is directly proportional to the forces exerted in the bridge system due to the earthquake ground motion. On the other hand, the sliding displacement of the super structure is crucial from the design point of view of the isolation system and the expansion joints.[13] Residual displacement is the displacement of the isolator relative to the displacement of the pier at the end of earthquake. For isolation to be effective, residual displacement is needed to be minimal. Residual displacement equal to zero ensures that the superstructure comes to its original position at the end of earthquake. In the first step, the performance of the VRFPS isolator considered for the present study without the VFD is compared with the performance of the FPS isolator without the VFD to investigate the advantages of the proposed VRFPS isolator system with a conventional FPS. In the next step, the effect of adding a VFD to the VRFPS isolator is studied. The performance of the VRFPS with a VFD is also compared with the performance of the FPS with a VFD to investigate the relative advantages of a VRFPS over a FPS after adding additional damping using the VFD. A parametric study by varying the damping coefficient

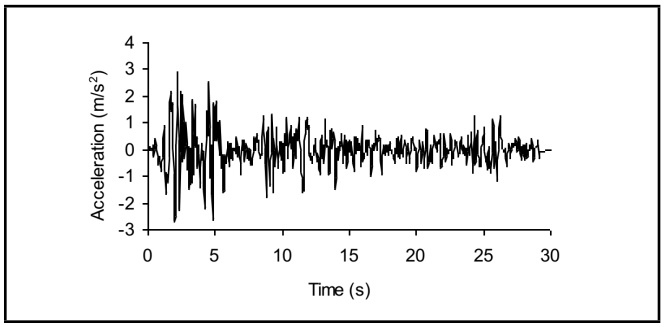

Figure 3a. El Centro earthquake.

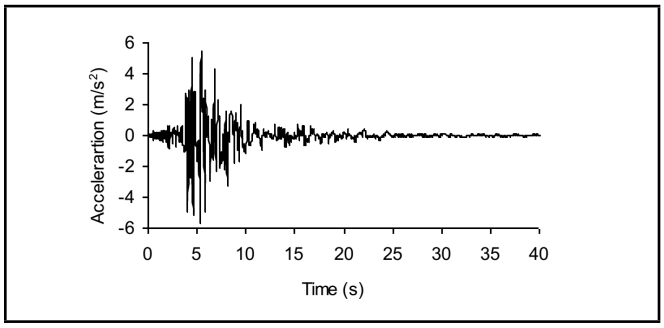

Figure 3b. Northridge earthquake.

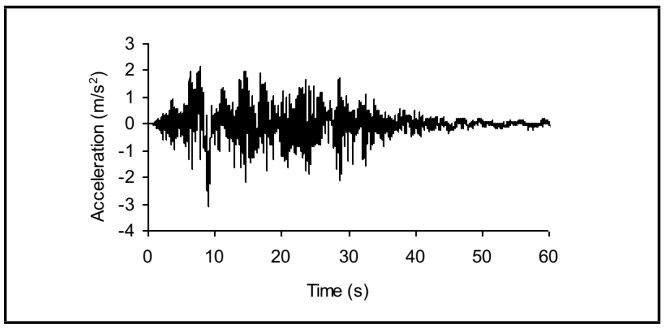

Figure 3c. Chi-Chi earthquake.

of the VFD is also carried out to investigate the efficiency of the proposed system for various values of the damping coefficients. For this, the performance of the VRFPS with a VFD is compared with the performance of the FPS with a VFD at various damping coefficients of the VFD.

4.1. Effect of Geometry of the Sliding Surface

The geometrical property of the proposed isolator is defined by the isolator constant, C, in Eq. (1). The effect of C on the performance of the isolator is studied for the Chi-Chi earthquake ground motion. Figure 4 shows the peak response of the base shear, sliding displacement, and residual displacement for various values of C. As shown in the figure, the base shear is comparatively larger and the residual displacement is nearly equal to zero at lower values of C. The base shear decreases, and the residual displacement increases with an increase in the value of C. The sliding displacement is comparatively larger for the values of C, ranging from 5 to 50. Based on the criteria of a low base shear and a small residual displacement, the value of C from 50 to 200 is recommended for the proposed isolator. For the present analysis, the value of C equal to 100 is considered.

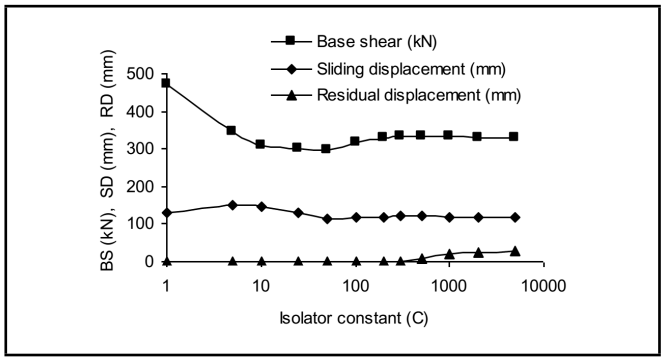

Figure 4. Variation of response with isolator constant.

4.2. Time History Response of the Isolated Bridge without VFD

The time history response obtained for a bridge structure isolated with a VRFPS only (i.e. without VFD) is presented in Figs. 5a, 5b, 5c, and 5d. For comparison, the time history response of a bridge isolated with a FPS without the VFD is also shown in the same figures. In this case, the response for the El Centro earthquake is obtained for two cases. The first case is for the recorded ground acceleration (medium intensity) whereas for the second case, the recorded ground acceleration is multiplied by an intensity factor of 2.0 (high intensity). Comparison of the response of the VRFPS with a FPS shows that the base shear is almost similar for both the systems for the El Centro earthquake of medium intensity whereas the bridge with the VRFPS experiences a significantly lower base shear for the high intensity El Centro earthquake, Northridge earthquake, and Chi-Chi earthquake. This indicates that the far-field excitations of high intensity and the near-fault excitations severely affect the performance of the FPS isolator. Interestingly, the peak base shear for the VRFPS is almost similar (varies from 223.2 kN–371.6 kN for VRFPS against 277.6 kN–682.9 kN for FPS) for all the four excitations, clearly demonstrating the advantages of the VRFPS to overcome the resonance problem that occurs in a FPS and its effectiveness for excitations of high intensity and for near-fault earthquakes. The time history response of sliding displacement shows a slightly larger maximum displacement for the VRFPS compared to the FPS. However, the residual displacement for both the systems is identical and is almost equal to zero, clearly demonstrating their ability to bring the structure to its original position. Thus, it is evident that the VRFPS isolator is more effective than the FPS isolator since the VRFPS reduces the base shear significantly for high intensity and near-fault earthquakes without much of an increase in the sliding displacement. The VRFPS is also effective in restoring the structure to its original position.

4.3. Time History Response of the Isolated Bridge with the VFD

It may be noted from the Figs. 5b, 5c, and 5d that the structure isolated with the VRFPS and FPS isolators slides considerably during the earthquake. Moreover, the sliding displacement of the VRFPS isolator is larger than that of the FPS isolator. For the isolation to be effective, the sliding displacement is to be within the limit. Hence, to reduce the sliding displace-

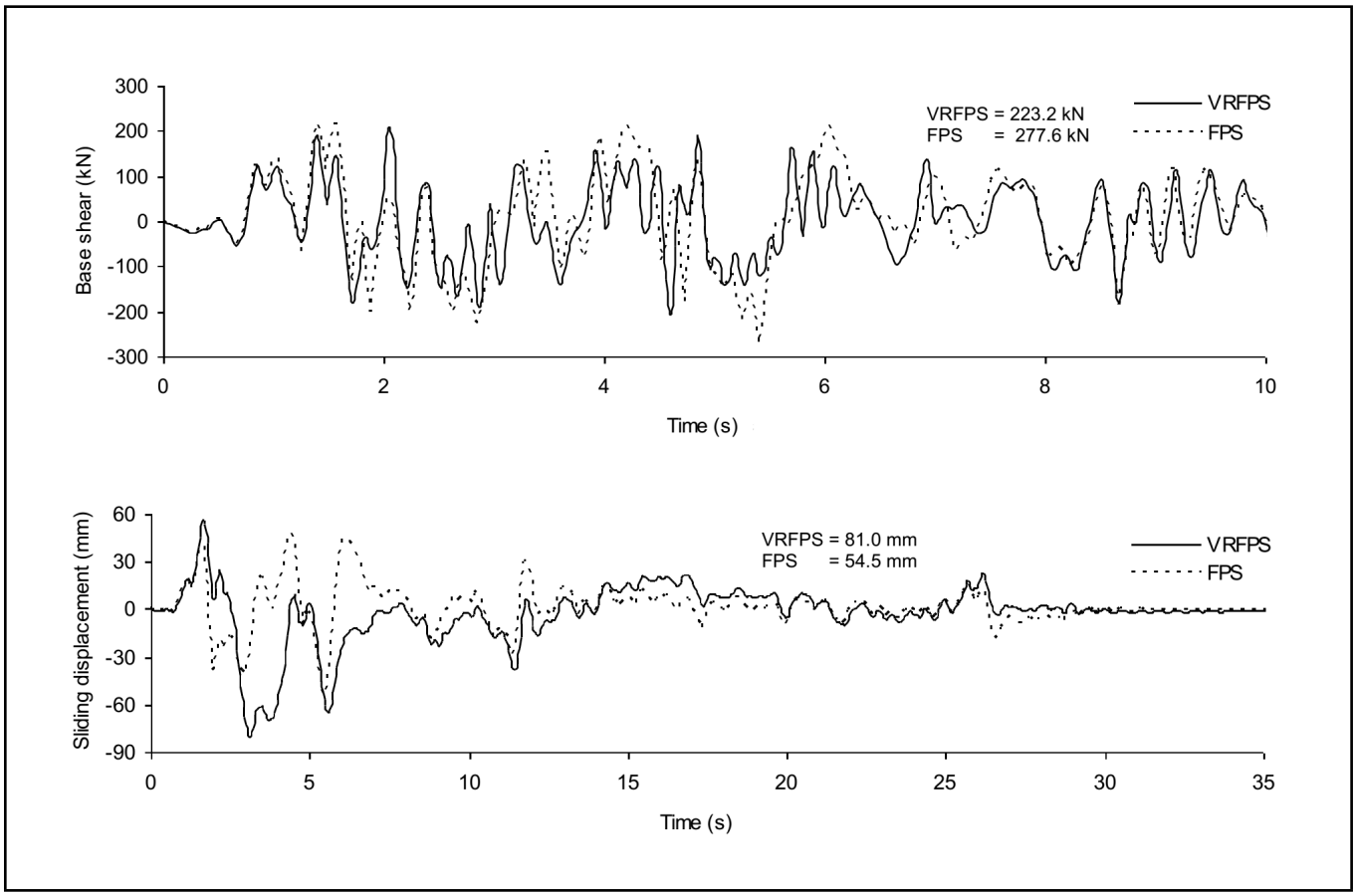

Figure 5a. Response of isolated bridge without VFD to El Centro earthquake of medium intensity.

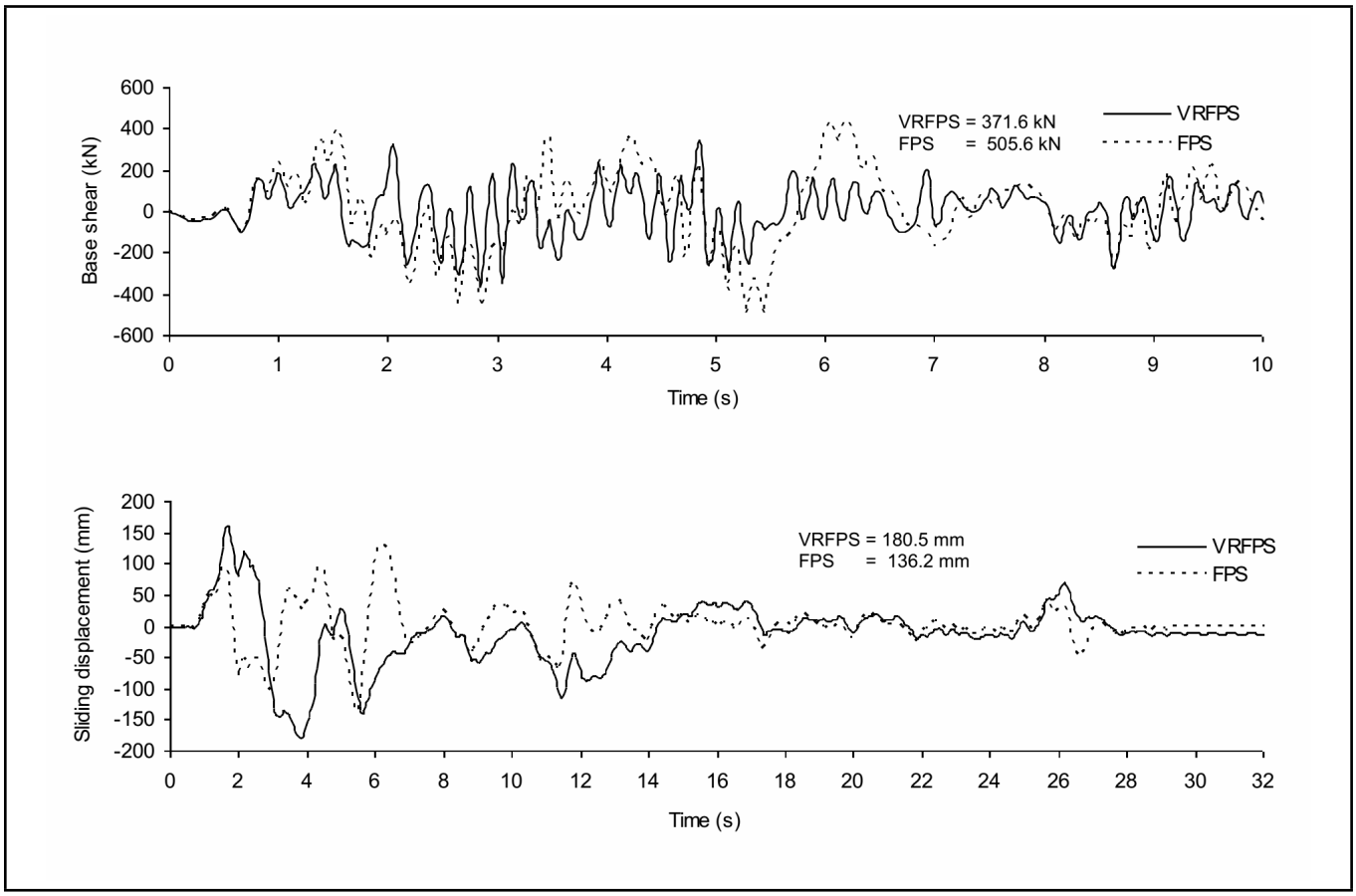

Figure 5b. Response of isolated bridge without VFD to El Centro earthquake of high intensity.

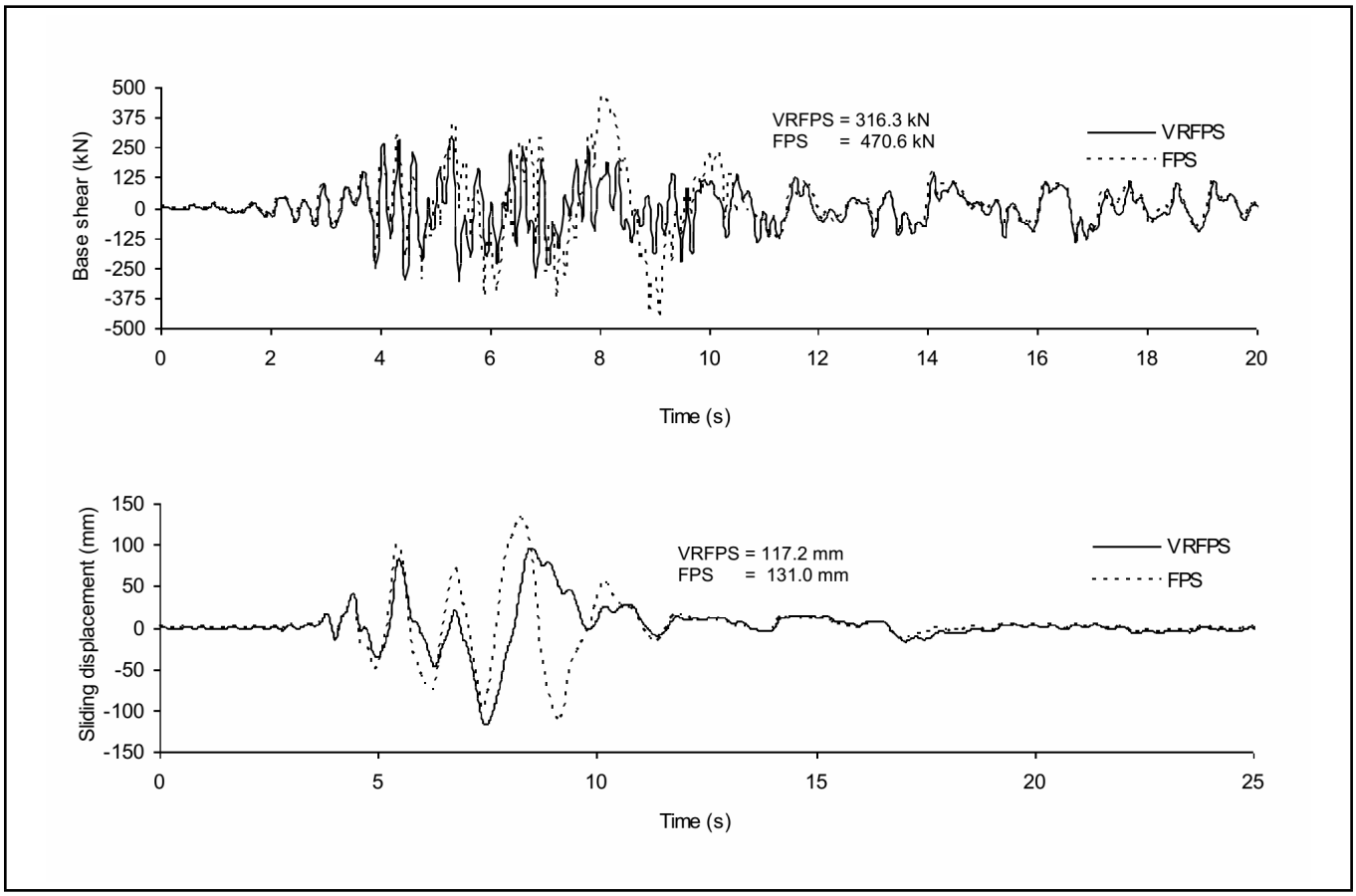

Figure 5c. Response of isolated bridge without VFD to Northridge earthquake.

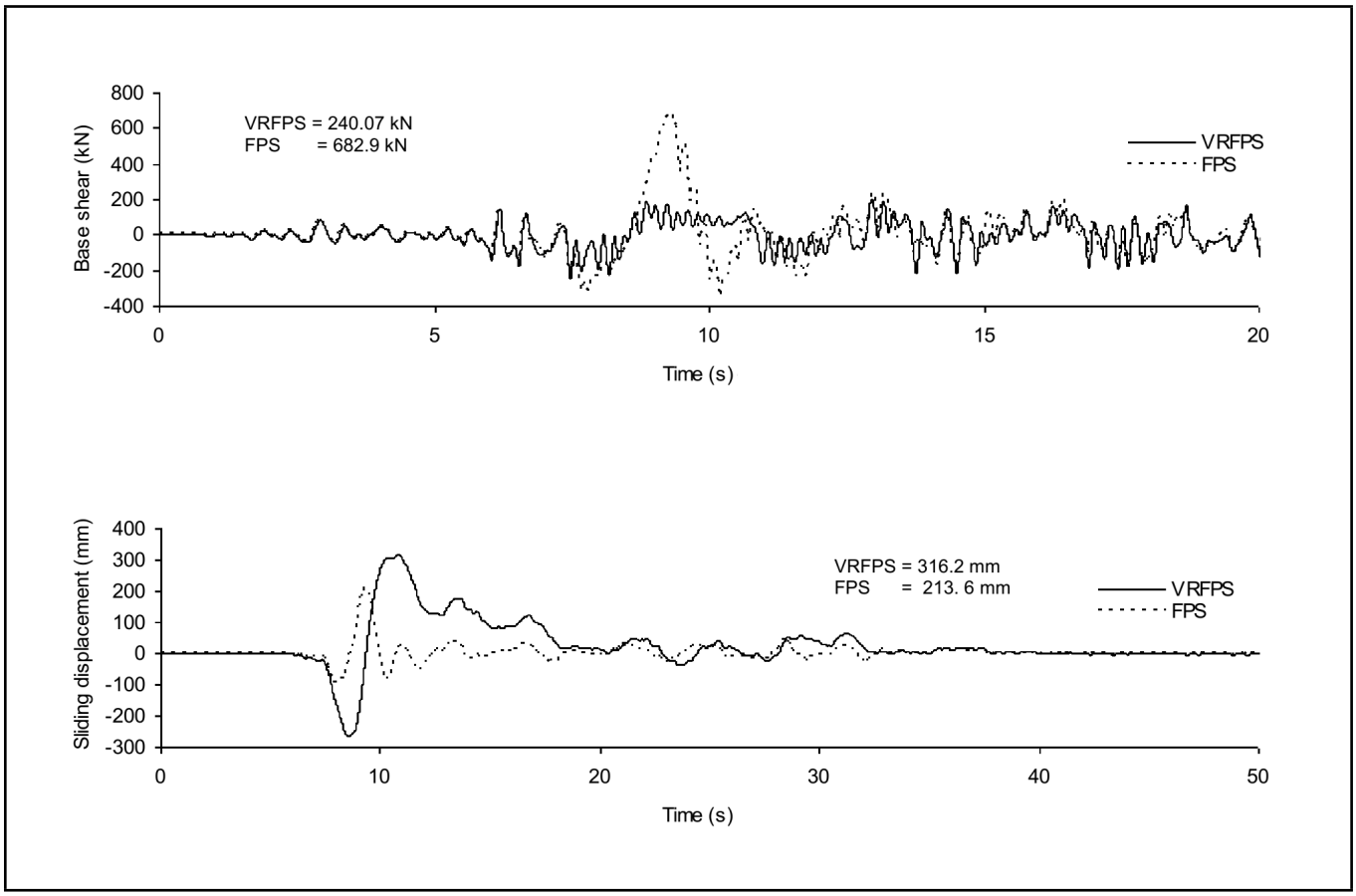

Figure 5d. Response of isolated bridge without VFD to Chi-Chi earthquake.

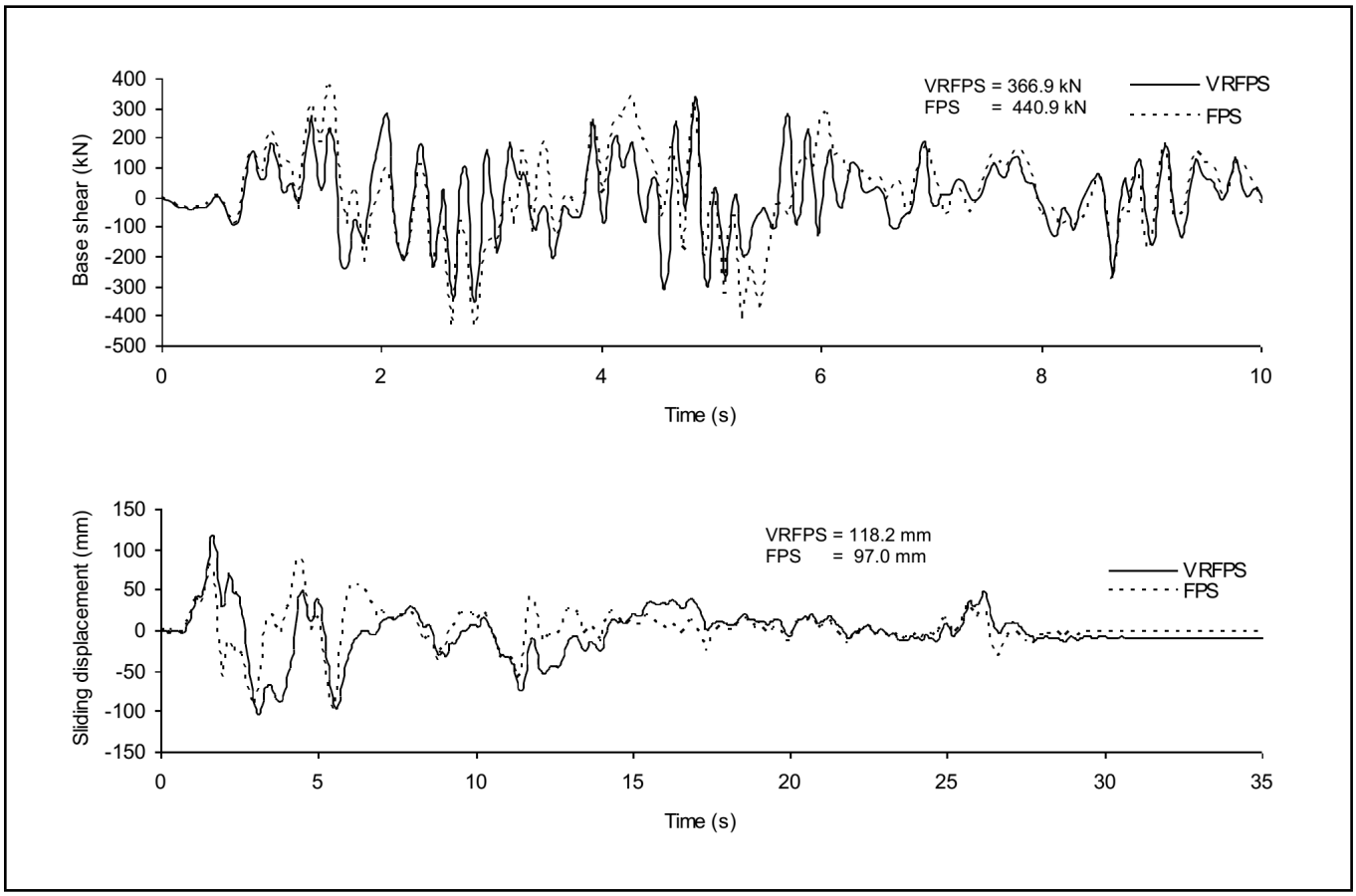

Figure 6a. Response of isolated bridge with VFD to El Centro earthquake of high intensity.

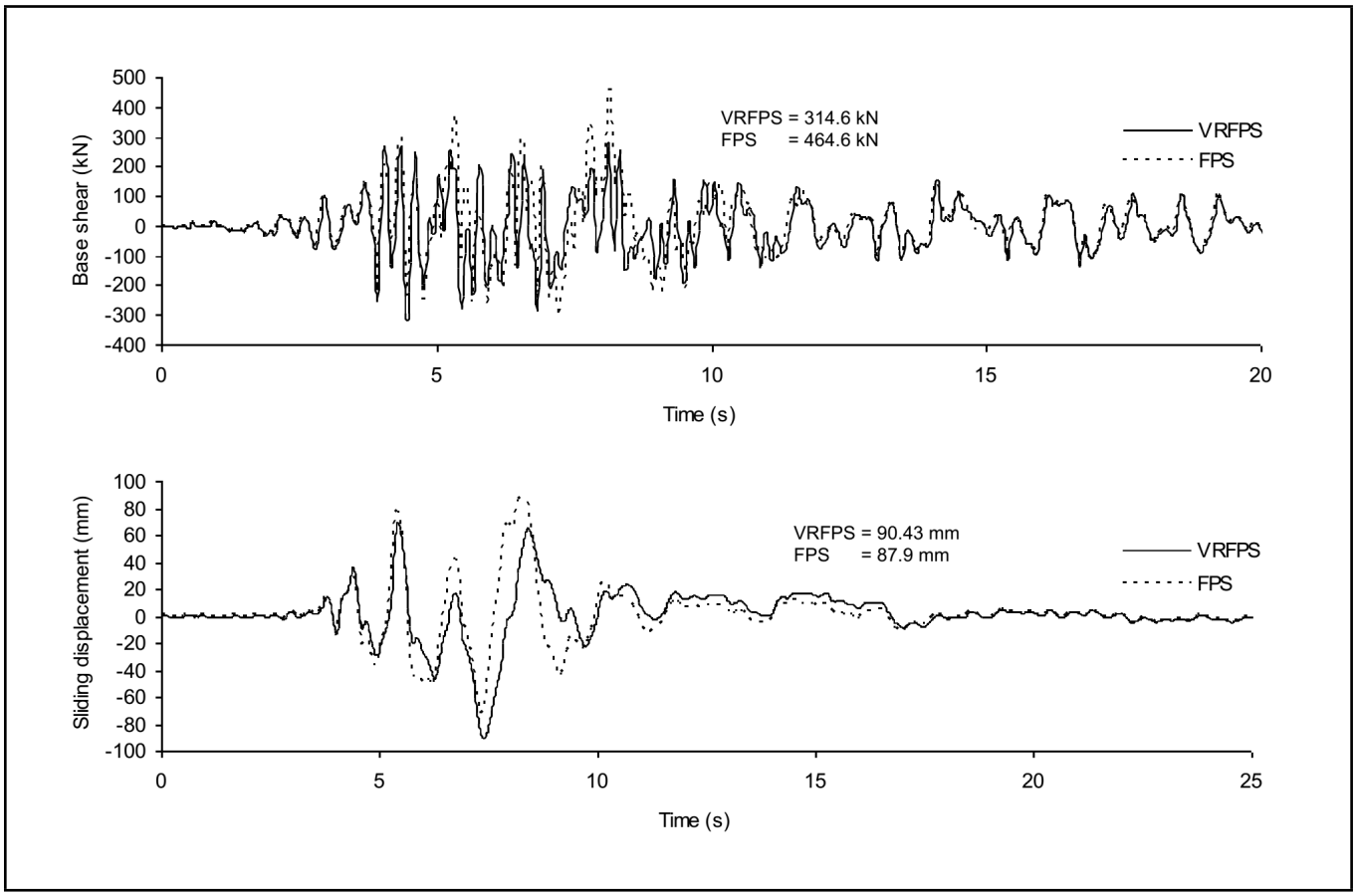

Figure 6b. Response of isolated bridge with VFD to Northridge earthquake ground motion.

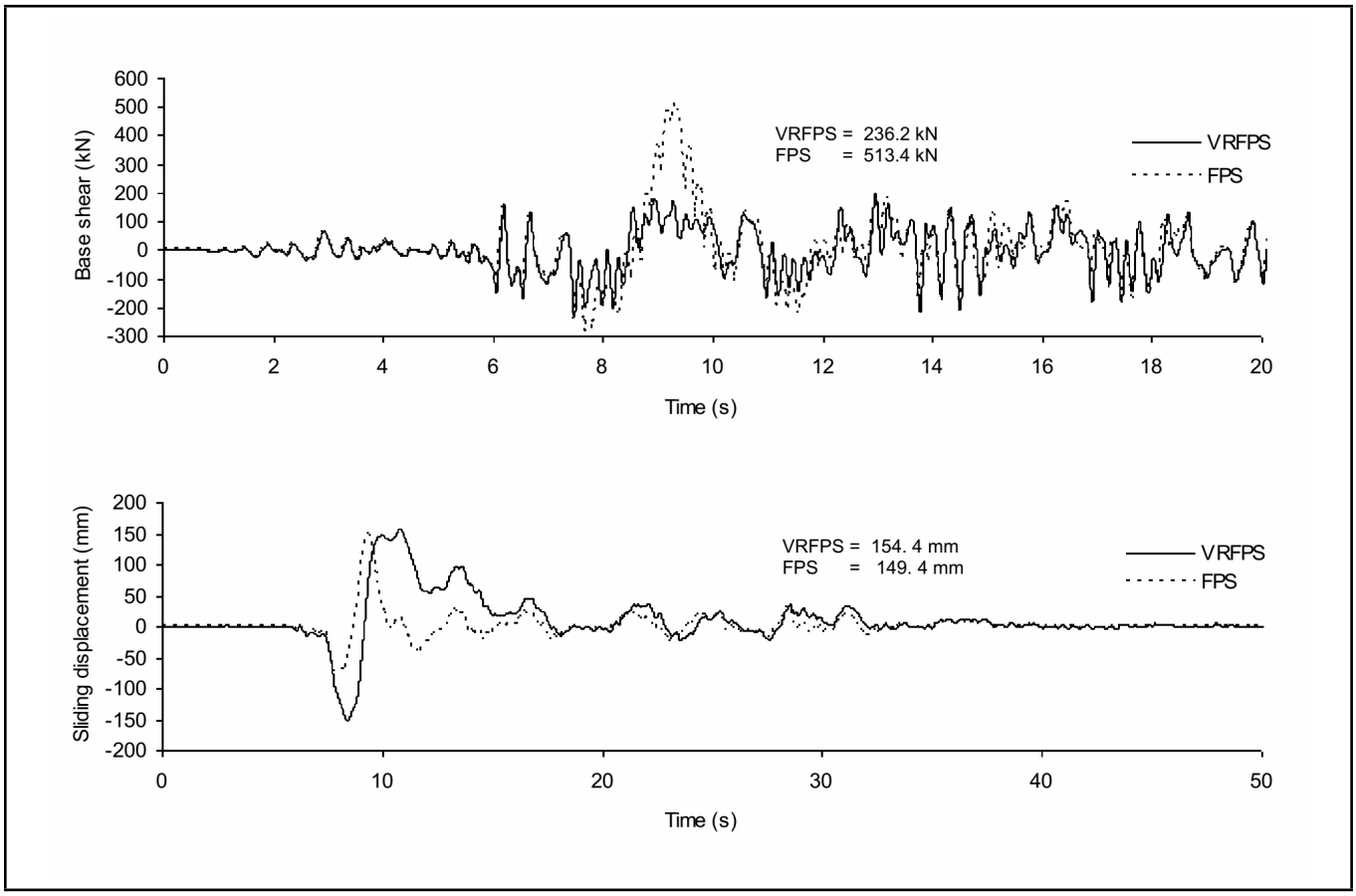

Figure 6c. Response of isolated bridge with VFD to Chi-Chi earthquake.

ment, a VFD system is placed between the superstructure and abutment, as already explained. The damping coefficient equal to 400 kNs/m is considered for the VFD. The time history response of the isolated bridge with the VFD system is shown in Figs. 6a, 6b, and 6c. It can be observed from the Figs. 5b, 5c, and 5d, and Figs. 6a, 6b, and 6c that the reduction in the displacement response is remarkable for the isolated bridge due to the addition of a passive hybrid system. Without the VFD, the sliding displacement of the VRFPS is larger than that of the FPS for the El Centro and the Chi-Chi earthquakes whereas for the Northridge earthquake, the sliding displacement of the FPS is larger than that of the VRFPS. However, the sliding displacement of both the systems is almost similar when additional passive damping is added for the VRFPS and the FPS isolators. The base shear reduces slightly due to the addition of the VFD for the FPS whereas for the VRFPS, the base shear will not change much due to the addition of the VFD. Overall, it can be observed from the time history plot of Figs. 6a, 6b, and 6c that the base shear of the bridge with the VRFPS is considerably lesser than that of the bridge with a FPS at an almost similar sliding displacement. Hence, again, a hybrid system consisting of the VRFPS and the VFD is more effective than a hybrid system consisting of the FPS and the VFD since the base shear of the bridge with the VRFPS is considerably lesser than that of a bridge with the FPS at an almost similar sliding and residual displacement when a passive hybrid, a VFD system, is added. The combined property i) variable frequency of the FPS and ii) additional damping of the VFD is effective to reduce the base shear of the FPS without increasing the sliding and residual displacement.

4.4. The Seismic Response of an Isolated Bridge with the VFD for a Various Damping Coefficient of the VFD

The effectiveness of a hybrid system consisting of the VRFPS isolator and the VFD to isolate the bridge structure is investigated for various values of the damping coefficient of the VFD. In addition to the base shear, sliding displacement, and residual displacement, the effectiveness of the proposed system for deck acceleration (acceleration of superstructure) is also investigated in this study. In the case of bearings with additional viscous dampers, relatively large forces may develop in dampers, and correspondingly large forces may be transmitted through the damper connections to the abutments and superstructure. Hence, the effect of the damping coefficient on the damping force is also considered for this study. Also, in this case, the response of the VRFPS is compared with the response of the pure friction (PF) system. Figures 7a, 7b, and 7c show the base shear, deck acceleration, sliding displacement, damping force, and residual displacement for various values of the damping coefficient. The damping coefficient of the VFD is varied from 0 to 1000 kNs/m. The corresponding variation of the damping ratio is from 0 to 0.9 for the FPS isolator. It may be noted that due to the variation in stiffness with sliding displacement, the damping ratio is not constant for the VRFPS during the earthquake. Hence, the responses in these figures are plotted in terms of the damping coefficient instead of the damping ratio. In these figures the response of the bridge at a zero damping coefficient corresponds to the response of the bridge isolated only with the VRFPS isolator (i.e. without the

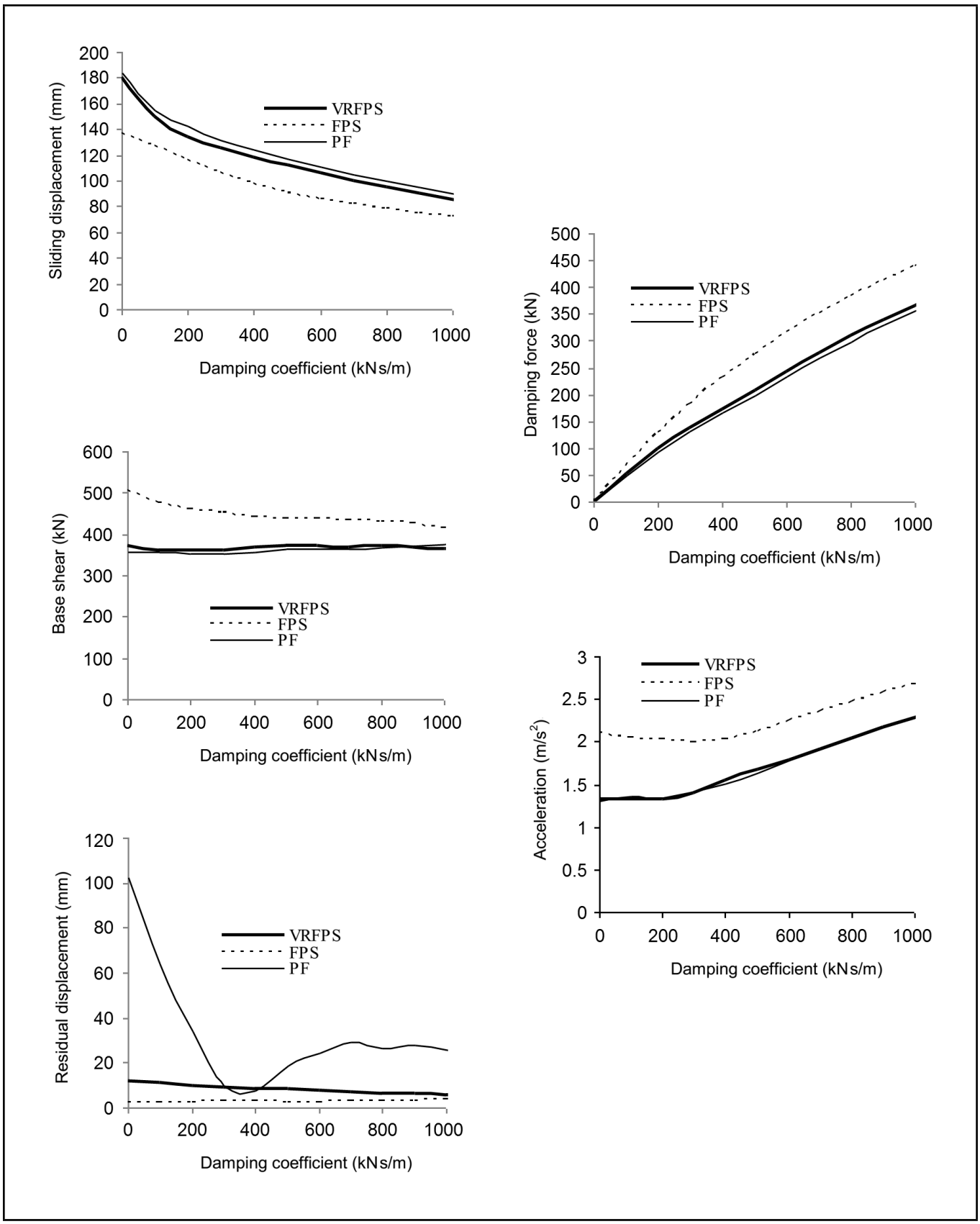

Figure 7a. Variation of response with damping coefficient for El Centro earthquake of high intensity.

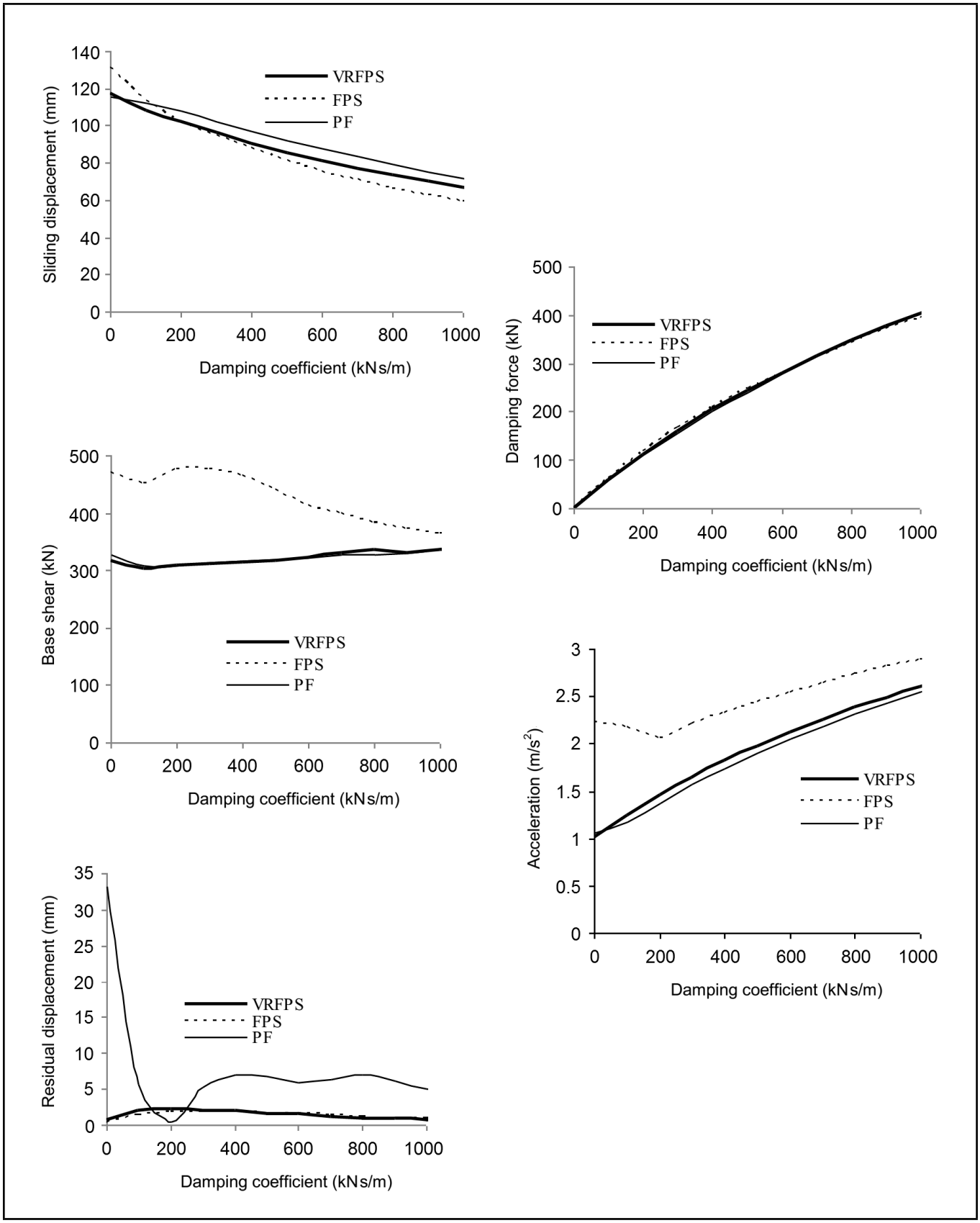

Figure 7b. Variation of response with damping coefficient for Northridge earthquake.

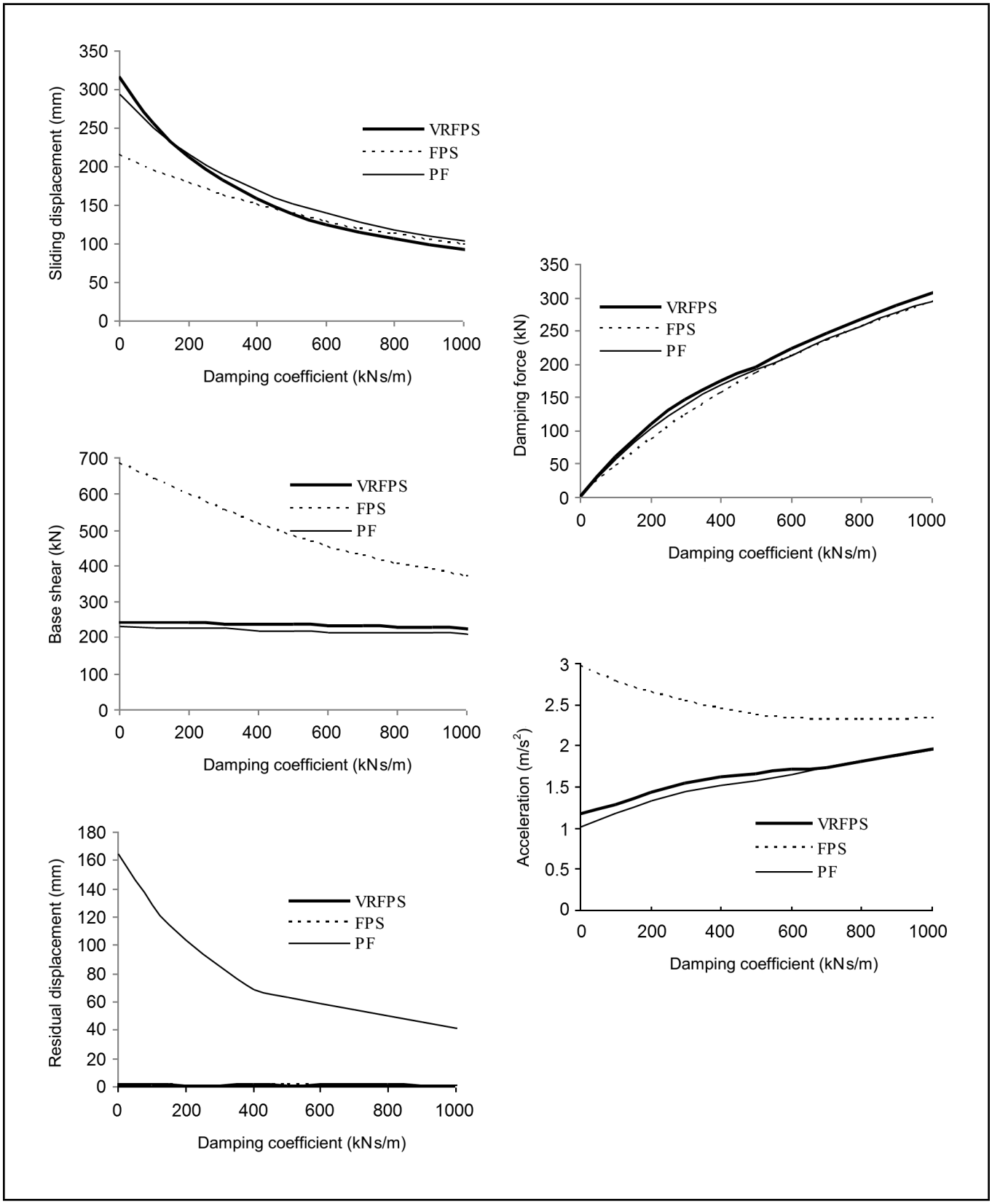

Figure 7c. Variation of response with damping coefficient for Chi-Chi earthquake.

VFD). From Figs. 7a, 7b, and 7c, the significant characteristic of all the three isolators is the sharp reduction in the sliding displacement with the damping coefficient. Without the passive damping system, the sliding displacement of the VRFPS is more than that of the FPS for the El Centro and Chi-Chi earthquake whereas for the Northridge earthquake, the sliding displacement of the FPS is more than that of the VRFPS. However, at a damping coefficient of about 400 kNs/m (corresponding to the damping ratio of 0.3 for FPS), the sliding displacement of both the isolators is almost similar. The response of the base shear shows that the base shear for the FPS decreases with an increase in the damping coefficient, reaches a minimum value, and then remains almost constant. However, for the VRFPS, the base shear will not vary much with the damping coefficient. The deck acceleration for the FPS initially decreases marginally, reaches a minimum value, and then increases with a further increase in the damping coefficient. The deck acceleration for the VRFPS, however, increases with an increase in the damping coefficient and is lesser compared to the deck acceleration of the FPS for all the values of the damping coefficient. Thus, combining the response of the base shear, deck acceleration, and sliding displacement, it is noteworthy that, for the damping coefficient more than about 400 kNs/m, the base shear and the deck acceleration of the VRFPS is considerably lesser than that of the FPS at an almost similar sliding displacement. The response of the VRFPS and the PF system shows that the base shear, deck acceleration, and sliding displacement of both the PF and the VRFPS are almost similar. However, the residual displacement is considerably larger for the PF system than that of the VRFPS. The VRFPS brings the structure to its original position whereas, the structure isolated with the PF system displaces considerably from its original position after the earthquake. The response of the damping force at various damping coefficients shows that the damping force increases with the damping coefficient, and the variation of the damping force with the damping coefficient is similar for all the three types of isolators.

5. CONCLUSIONS

The effectiveness of a variable radius friction pendulum system (VRFPS) with an additional passive viscous fluid damper (VFD) to control the seismic response of a continuous bridge is studied. The performance of the proposed isolator is compared with the performance of a conventional friction pendulum system (FPS) and a pure friction (PF) system. The VRFPS does not show any resonance problem that occurs in a FPS for near-fault earthquake ground accelerations. However, the sliding displacement of the VRFPS is slightly more than the sliding displacement of the FPS due to the relatively flatter surface of the VRFPS than the FPS at a large sliding displacement. By adding a passive VFD system to the VRFPS, the sliding displacement decreases considerably, and its effectiveness increases further. In this case, the sliding displacement of both the FPS and the VRFPS systems is similar but the base shear and the deck acceleration for the VRFPS is considerably lesser than that of the FPS. Similar to the FPS, the VRFPS is also effective in bringing the structure to its original position after the earthquake. The base shear, deck acceleration, and sliding displacement of the VRFPS is similar to the PF system. However, the residual displacement of the PF system is considerably larger than the VRFPS. The VRFPS has the advantages of both the FPS and the PF system.

REFERENCES

[1] Zayas, V. A., Low, S. S., and Mahin, S. A. A simple pendulum technique for achieving seismic isolation, *Earthquake Spectra*, **6** (2), 317–333, (1990).

[2] Pranesh, M. and Sinha, R. VFPI: an isolation device for aseismic design, *Earthquake Engineering & Structural Dynamics*, **29** (5), 603–627, (2000).

[3] Lu, L. Y., Wang, J., and Hsu, C. C. Sliding isolation using variable frequency bearings for near-fault ground motions, *Proc. of the fourth International Conference on Earthquake Engineering*, Taipei, Taiwan, (2006).

[4] Tsai, C. S., Chiang, T. C., and Chen, B. J. Finite element formulations and theoretical study for variable curvature friction pendulum system, *Engineering Structures*, **25** (14), 1719–1730, (2003).

[5] Tsopelas, P. C., Constantinou, M. C., Okamota, S., Fujii, S., and Ozaki, D. Experimental study of bridge seismic sliding isolation systems, *Engineering Structures*, **18** (4), 301–310, (1996).

[6] Soneji, B. B. and Jangid, R. S. Passive hybrid systems for earthquake protection of cable-stayed bridge, *Engineering Structures*, **29** (1), 57–70, (2007).

[7] Symans, M. D. and Kelly, S. W. Fuzzy logic control of bridge structures using intelligent semi-active seismic isolation systems, *Earthquake Engineering & Structural Dynamics*, **28** (1), 37–60, (1999).

[8] Yoshioka, H., Ramallo, J. C., and Spencer, B. F. "Smart" base isolation strategies employing magnetorheological dampers, *Journal of Engineering Mechanics*, **128** (5), 540–551, (2002).

[9] Kim, H. S. and Roschke, P. N. Design of fuzzy logic controller for smart base isolation system using genetic algorithm, *Engineering Structures*, **28** (1), 84–96, (2006).

[10] Jung, H. J., Choi, K. M., Spencer, B. F., and Lee, I. W. Application of some semi-active control algorithms to a smart base-isolated building employing MR dampers, *Structural Control and Health Monitoring*, **13** (2–3), 693–704, (2006).

[11] Lu, L. Y., Lin, G. L., and Kuo, T. C. Stiffness controllable isolation system for near-fault seismic isolation, *Engineering Structures*, **30** (3), 747–765, (2008).

[12] Krishnamoorthy, A. Variable curvature pendulum isolator and viscous fluid damper for seismic isolation of structures, *Journal of Vibration and Control*, **17** (12), 1779–1790, (2011).

[13] Jangid, R. S. Stochastic response of bridges seismically isolated by friction pendulum system, *Journal of Bridge Engineering*, **13** (4), 319–330, (2008).